Agricultural and Forest Meteorology 300 (2021) 108318

Contents lists available at ScienceDirect

Agricultural and Forest Meteorology

journal homepage: www.elsevier.com/locate/agrformet

Precipitation rather than evapotranspiration determines the warm-season water supply in an alpine shrub and an alpine meadow

Hongqin Li [a,b,1], Fawei Zhang [b,c,e,1,*], Jingbin Zhu [b,f,1], Xiaowei Guo [b], Yikang Li [b], Li Lin [b], Leiming Zhang [d], Yongsheng Yang [b], Yingnian Li [b,*], Guangmin Cao [b,*], Huakun Zhou [b,c], Mingyuan Du [g]

[a] College of Life Sciences, Luoyang Normal University, Luoyang, Henan, 471934, China
[b] Key Laboratory of Adaptation and Evolution of Plateau Biota, Northwest Institute of Plateau Biology, Chinese Academy of Sciences, Xining, Qinghai, 810001, China
[c] Qinghai Provincial Key Laboratory of Restoration Ecology in Cold Region, Northwest Institute of Plateau Biology, Chinese Academy of Sciences, Xining, Qinghai, 810001, China
[d] Synthesis Research Center of Chinese Ecosystem Research Network, Key Laboratory of Ecosystem Network Observation and Modeling, Institute of Geographic Sciences and Natural Resources Research, Chinese Academy of Sciences, Beijing, 100101, China
[e] Institute of Sanjiangyuan National Park, Chinese Academy of Sciences, Xining, Qinghai, 810001, China
[f] College of Tourism, Resources and Environment, Zaozhuang University, Zaozhuang, Shandong, 277100, China
[g] Institute for Agro-Environmental Sciences, National Agriculture and Food Research Organization, Tsukuba, 305-8604, Japan

ARTICLE INFO

Keywords:
Eddy covariance techniques
Evapotranspiration
Water supply
Bulk surface resistance
Atmospheric evaporative demand
Qinghai-Tibetan plateau

ABSTRACT

Alpine regions are generally referred to as water towers for the lowlands, yet the water balance has not been quantified for alpine catchments with different vegetation types. This paper presented a multi-year time series of evapotranspiration (ET) and water supply (precipitation minus ET) during the warm-season (June to September), measured using eddy covariance techniques for an upper alpine shrub (3400 m) and for a lower alpine meadow (3200 m), on the northeastern Qinghai-Tibetan Plateau. The monthly ET for the shrub averaged 71.8 ± 10.1 mm (Mean ± SD), which was 22.7% lower than for the meadow. ET peaked at 89.0 ± 3.0 mm for the shrub and at 113.9 ± 2.6 mm for the meadow both in July. The monthly water supply was nearly neutral from June to July and represented a surplus in August and September at both sites. The mean warm-season ET and water supply were 287.0 ± 17.6 mm and 59.6 ± 16.3 mm for the shrub, and 352.2 ± 15.7 mm and 22.5 ± 32.5 mm for the meadow, respectively. Piecewise structural equation models showed that variability of daily ET was dominated more by net radiation (R_n) than by vapor pressure deficit (VPD) at both sites. However, net radiation was 32.6% higher for the shrub than for the meadow, but this did not drive higher ET for the shrub. This was explained by the difference in the energy partitioning strategy (Bowen ratio), which was attributable to the difference in the bulk surface resistance, rather than the difference in the climatological resistance (which is proportional to VPD/R_n). The seasonal and annual variability of water supply was determined by precipitation rather than by ET. The linear slopes of water supply with precipitation were all close to one, regardless of vegetation type. This suggested that the water yield efficiency was consistent at the two sites. Our results highlighted the different effects of vegetation type on ET and water supply for humid alpine regions. The lower ET loss and consequent higher water yield, but with less digestible forage in the shrub, would present a dilemma for the balance between water supply and forage production under current shrub expansion in alpine rangeland.

1. Introduction

Cold regions, including areas with permafrost, glaciers, and stable seasonal snow cover, occupy 43.5% of China's land surface and are generally referred to as "water towers for Asia" because they occur at the headwaters of most large rivers in Asia (Chen et al., 2006; Yao et al., 2012). Evapotranspiration (ET) over cold land is critical to hydrological cycle and energy exchange, and strongly affects the regional water

* Corresponding authors at: 23, Xinning Streets, Xining, Qinghai, 810001, China.
E-mail addresses: mywing963@126.com (F. Zhang), ynli@nwipb.cas.cn (Y. Li), caogm@nwipb.cas.cn (G. Cao).
[1] These authors contribute equally

https://doi.org/10.1016/j.agrformet.2021.108318
Received 21 July 2020; Received in revised form 24 November 2020; Accepted 2 January 2021
Available online 11 January 2021

balance and atmospheric circulation, through land-atmosphere feedbacks (Baldocchi et al., 2004; Teuling et al., 2010; Peng et al., 2019). The terrestrial water supply depends on a balance between precipitation inputs and ET losses (Wieser et al., 2008; Chapin et al., 2011; Zuo et al., 2016). This balance is crucial for water availability in lowland areas, and is closely related to surface conditions and atmospheric evaporative demand, however details of ecohydrological processes in alpine areas are not well understood (Kelliher et al., 1993; McFadden et al., 2003; Yang et al., 2012). Moreover, alpine areas have been experiencing a rapidly warming climate, which has resulted in changes to the land cover, such as shrub expansion, surface greening, and grassland degradation. These changes could substantially influence the timing and magnitude for ET and water cycle (ACIA, 2004; Blok et al., 2011; Liljedahl et al., 2011; Zeng et al., 2017) via changes in the surface roughness, leaf area index, available energy (incorporating albedo), and available water at the land surface (Sterling et al., 2013; Shen et al., 2015). Understanding the mechanisms and environmental factors that constrain ET and water supply in alpine regions is therefore crucial for robust projections of regional weather and effective management of downstream water resources (Wilson et al., 2002; Li X et al., 2014; Rydsaa et al., 2015; Biskop et al., 2016).

The canopy-scale "big-leaf" paradigm shows that, under moist conditions, terrestrial ET is regulated by atmospheric evaporative demand and surface water vapor resistance (Monteith, 1965; Kelliher et al., 1993; Baldocchi and Xu, 2007). Previous studies have reported the competing roles of radiation energy availability (Humphreys et al., 2006; Knowles et al., 2012; Zhang et al., 2018), the saturated vapor pressure deficit (McFadden et al., 2003; Hammerle et al., 2008; Liljedahl et al., 2011), and the surface moisture status (Gu et al., 2005; 2008; Zhu et al., 2014), for driving spatiotemporal variability in ET in vegetated alpine areas during the warm-season (June to September). The relative importance of ET and precipitation for the water supply depends on whether ET is demand-limited or supply-limited, which is likely to vary with vegetation type and climate (Gu et al., 2008; Wieser et al., 2008; Xiao et al., 2013). The relative contributions of abiotic and biotic controls to ET and water supply variability, and the potential biophysical mechanisms, have not well been quantified (Baldocchi et al., 2004; Hu et al., 2009; Chapin et al., 2011; Brümmer et al., 2012; Zhang et al., 2016). The different processes that determine ET and water supply across alpine grasslands are closely linked to the energy partitioning strategy, which can be described using the ratio of the sensible heat flux to the latent heat flux; the so-called Bowen ratio. The partitioning strategy is closely related to the bulk surface resistance (r_s) and the consequent plant water use tactic (Eugster et al., 2002; Wilson et al., 2002; McFadden et al., 2003). r_s reflects the integrated resistance of canopy plant stomata and soil vapor transfer, and responds to short-term changes in the atmospheric evaporative demand and the soil moisture status, and can, in turn, indicate ET (Wilson et al., 2002; McFadden et al., 2003; Baldocchi and Xu, 2007). This loop feedback between energy partitioning and ecohydrological processes can constrain model projections of water dynamics and budgets in alpine vegetated areas (Hammerle et al., 2008; Williams et al., 2012). However, process-driven regional models cannot be quantitatively validated for alpine areas partly because of the absence of long-term field measurements with different vegetation types (Konzelmann et al., 1997; Hu et al., 2009; Xiao et al., 2013; Biskop et al., 2016). Hence, a mechanistic understanding of controls on the spatiotemporal patterns of ET and water supply derived from long-term observations of alpine catchments with different vegetation types should improve our knowledge of key ecohydrological processes and reduce uncertainties in the modeling water supply.

Alpine shrub and alpine meadow are common vegetation types and often co-exist in humid alpine climates, with the former usually growing at higher elevations than the latter (Konzelmann et al., 1997; Zheng et al., 2000). Variations in ET and the water supply have been reported to be the result of the competing abiotic roles of precipitation (Gu et al., 2008; Biskop et al., 2016) and net radiation (Wieser et al., 2008; Zhang et al., 2016; 2018) in humid alpine regions. Vegetation type (Hu et al., 2009; Zuo et al., 2016) and associated abundance of moss (Blok et al., 2011; Liljedahl et al., 2011) could account for a significant proportion of ecosystem-scale hydraulic diversity (Anderegg et al., 2018), and thus for variations in water use strategy, spatiotemporal ET and water supply (Eugster et al., 2002; Humphreys et al., 2006; Teuling et al., 2010). It is therefore important to understand the relative importance of abiotic and biotic controls on ET and the water supply. We analyzed a multi-year time series of ET observations in the warm-season over an upper shrub area of *Potentilla fruticosa* (3400 m) and a lower meadow area of *Kobresia humilis* (3200 m) along a vegetated mountainside on the northeastern Qinghai-Tibetan Plateau. The key focus was to quantify the inter- and intra-annual variability for ET and the water supply, and to explore the relative contributions of abiotic drivers and vegetation controls on the variability. Although it is widely accepted that ET rates are largely controlled by the available radiation energy at humid sites, we hypothesized that ET has some dependence on vegetation type, because the canopy structure over alpine shrub areas is different to that over alpine meadow areas. Our results also provide field information that explains the responses of ET and water supply to the current vegetation shift from alpine meadow to alpine shrub in some areas (Eugster et al., 2002; Klein et al., 2007). This evidence helps to resolve inconsistencies between numerical modeling results and the micro-lysimeter experimental findings, since the former suggested that shrub expansion had only a small effect on surface energy fluxes (Rydsaa et al., 2015), while the latter showed that shrub expansion influenced substantially on surface water exchanges (Blok et al., 2011).

2. Materials and methods

2.1. Site description

Field measurements were conducted near the Haibei National Field Research Station for Alpine Grasslands (Haibei Station, 37° 37′ N, 101° 19′ E, 3200 m a.s.l.), on the northeastern Qinghai-Tibetan Plateau, which is part of the China Flux Observation and Research Network (ChinaFlux). The site has a continental plateau climate, with a short warm wet summer from June to September, and a long cold dry winter for the rest of the year. From 2003 to 2017, the mean air temperature and precipitation were –1.1°C and 423.5 mm, respectively, in the shrub, and –0.5°C and 499.2 mm, respectively, in the meadow. A more detailed description of the climate is provided in Li et al (2015). Areas of alpine shrub and alpine meadow are common at elevations of 3300–3500 m and 3100–3300 m, respectively, throughout the study region (Fig. S1). Our two study sites are separated by ca. 8 km horizontal distance and both are moderately (3.75 sheep ha^{-1}) grazed by Tibetan sheep and yaks from mid-October to late May.

The shrub is comprised of two distinct layers: a shrub overstory and a grass understory. The overstory is deciduous *P. fruticosa*, with coverage and height of ca. 60%–80% and 30–60 cm. The grass understory commonly consists of *Kobresia humilis, Stipa aliena, Poa orinosa, Helictotrichon tibeticum, Elymus nutans, Aster flaccidus, Polygonum viviparum*, and *Leontopodium nanum*. The meadow is dominated by *K. humilis*, followed by *E. nutans, S. aliena, Taraxacum dissectum, Anaphalis lacteal*, and *P. anserine*. The plant abundance and canopy height for the alpine meadow peak in late July, at around 92–98% and 10–30 cm, respectively. The peak leaf area index (LAI) of herbaceous vegetation is 2.5 m^2 m^{-2} in the shrub and 3.9 m^2 m^{-2} in the meadow, respectively. The canopy was less dense over the shrub because *P. fruticosa* has sparse perennial branches and its leaf dimensions are small (ca. 0.8 cm × 0.3 cm). The landscape is somewhat heterogeneous in the shrub area, where extensive patches of vegetation are mixed with patches of bare soil and soil covered in moss that is less than ~1.0 cm thick. The canopy over the meadow is less open, due to the prostrate stature of the dominant herbaceous species. The root biomass is concentrated in the 0–20 cm soil

layer, which accounts for around 85% and 95% of the total root biomass for the shrub and the meadow, respectively. The soil is classified as Mollic Gryic Cambisols for the shrub, and Mat Cry-gelic Cambisol for the meadow. The physical properties and water holding capacity for the soil are shown in Table 1. The minimum groundwater level in the meadow was about 3.9 m and little exchanged with precipitation during the warm-season (Zhang et al., 2019).

2.2. Data collection and quality control

The measurements were conducted by open-path eddy-covariance systems during the warm-season (June–September) for 10 years (2003–2012) in the shrub, and for 4 years (2014–2017) in the meadow. At both field sites, the relatively flat terrain and adequate fetch create conditions that are close to ideal for measuring fluxes (Fig. S1). The eddy-covariance system consists of a three-dimensional ultrasonic anemometer (CSAT3, Campbell, USA) and a rapid infrared CO_2/H_2O gas analyzer (LI-7500 in the shrub at 2.5 m height and LI-7500A in the meadow at 2.2 m height; LI-Cor, USA). Routine meteorological measurements were made synchronously, including air temperature (T_a), relative humidity (RH, HMP45C, Vaisala, Finland), and wind velocity (W_s, 034A-L, RM Young, USA) at 2.5 m, net radiation (R_n, CNR4, Kipp & Zone, Netherlands) at 1.5 m, precipitation (Rain, 52203, RM Young, USA) at 0.5 m, and the 5 cm-depth soil heat flux (G, HFT-3, Campbell, USA), 10 cm-depth volumetric soil water content (SWC, CS616, Campbell for the shrub and HydraII, Stevens, USA for the meadow), and 10 cm-depth soil temperature (T_s, 105T, Campbell for the shrub and HydraII for the meadow). The average topsoil (0-10 cm) gravimetric water content by oven drying methods showed similar seasonal trends and an insignificant difference between the two sites (Fig. S2). This was consistent with the results of volumetric soil water content (Fig. 1). Inconsistency of the instruments used at the two sites therefore did not significantly affect the measured volumetric soil water content. Further details on the instruments were provided in Li et al (2016) for the shrub and in Zhang et al (2018) for the meadow. Each flux tower was protected from sheep and yaks by a wire fence that enclosed a 50 m × 50 m area. Satellite-derived vegetation indices were flux tower-centric at 250 m × 250 m spatial resolution and were obtained from the Oak Ridge National Laboratory Distributed Active Archive Center (ORNL DAAC, http://daac.ornl.gov/MODIS/modis.html). Some abnormal values for the vegetation indices (attributable to clouds) were discarded and temporally gap-filled. The 16-day enhanced vegetation index (EVI, MOD13Q1) and the normalized difference vegetation index (NDVI, MOD13Q1) were temporally interpolated into an 8-day resolution, to match the temporal resolution of LAI (MOD15A2H). The 8-day EVI was used for further analysis because the coefficient of determination (R^2) of the correlation between ET and EVI was higher than those of ET and LAI or NDVI (Fig. S3).

ET data were screened by removal of outliers (beyond 4.5 standard deviations) in a 10-day moving window and by applying a night-time low-velocity filter (threshold friction velocity was 0.15 m•s^{-1}) to improve data quality. The valid proportion of daytime and all-day flux data was about 80% and 63% in the shrub, 84% and 76% in the meadow, respectively. The daily energy closure ratio averaged 0.76 and 0.80 for the shrub and the meadow, respectively. Since the mechanisms for the lack of closure were not fully understood Wilson et al., 2002), and underestimation of the soil heat flux was the most significant source (ca. 10%) of uncertainty for calculated energy closure in alpine grasslands (Xin et al., 2018), no energy balance residual correction on ET was implemented in our study. The measured ET was only slightly lower than the reference ET for the shrub, and was higher than the reference ET for the meadow (Fig. 2), which suggested that the measured ET may approach the upper limit that is imposed by the atmospheric evaporative demand (Peng et al., 2019), and was therefore unlikely to be significantly underestimated during the warm-season. Gaps in ET data were filled by linear regression of ET with net radiation (Gu et al., 2005) in a gap-centric window of 10-day valid data. The aerodynamic resistance (r_a), Bowen ratio (β), midday bulk surface resistance (r_s, 9:00 to 16:00), and decoupling coefficient (Ω) have been calculated from Eqs. (1)–((4) in similar alpine studies (Gu et al., 2008; Zhang et al., 2018).

$$r_a = \frac{W_s}{u_*^2} + 6.2W_s^{-0.67} \tag{1}$$

$$\beta = \frac{H}{LET} = \frac{1 + (r_s/r_a) - (r_i/r_a)}{(\Delta/\gamma) + (r_i/r_a)} \tag{2}$$

$$r_s = \frac{\rho C_p(VPD)}{\lambda(LET)} + \left(\beta\frac{\Delta}{\gamma} - 1\right)r_a \tag{3}$$

$$\Omega = \frac{1 + \Delta/\gamma}{1 + \Delta/\gamma + r_s/r_a} \tag{4}$$

where W_s is the wind velocity (m s^{-1}), u_* is the friction velocity (m s^{-1}), ρ is the air density (kg m^{-3}), C_p is the specific heat of air at constant pressure (1013 J kg^{-1} K^{-1}), VPD is the saturated vapor pressure deficit (kPa), γ is the psychrometric constant (kPa K^{-1}), Δ is the slope of the saturation vapor pressure curve with respect to temperature (kPa K^{-1}), H is the sensible heat flux, LET is the latent heat flux (L is the latent heat of vaporization J kg^{-1}), R_n is the net radiation, G is the soil heat flux, r_i is the so-called climatological resistance (ρCp(VPD)/(γ(R_n-G))) (Wilson et al., 2002).

The reference ET (ET_0) was used to study the evaporative demand from the atmosphere, independently of vegetation types, and was calculated from the FAO-56 Penman-Monteith ET Equation (Eq. (5)) for a hypothetical area of well-watered grass, with a canopy at 0.12 m, an LAI of 4.8 m^2 m^{-2}, a bulk surface resistance of 70 s m^{-1}, and an albedo of 0.23 (Allen et al., 1998).

$$ET_0 = \frac{0.408\Delta(R_n - G) + \gamma\frac{900}{T_a+273}W_s(VPD)}{\Delta + \gamma(1 + 0.34W_s)} \tag{5}$$

A small number of unrealistically high values, attributable to rain or dew events, were discarded (McFadden et al., 2003). Half-hourly values for ET and the environmental controls were aggregated into 8-day values.

2.3. Statistical analysis

ET and main factors were averaged over the 8-day serials to reduce day-to-day variability (leap year 8-day serials were neglected and

Table 1
Soil texture, bulk density and water holding capacity in the shrub and in the meadow.

Site	Soil depth /cm	Soil texture 2–0.05 mm / %	0.05–0.002 mm / %	<0.002 mm / %	Bulk density /g cm^{-3}	Saturated water /mm	Field water /mm	Wilting water /mm	Specific water capacity* / mm hPa^{-1}
Shrub	0–20	14.0	77.75	8.25	0.62	178.19	123.50	19.10	1.05
	20–40	9.70	84.90	5.40	1.12	178.75	118.94	18.14	1.28
Meadow	0–20	44.45	49.30	6.25	0.72	150.34	77.18	18.00	0.50
	20–40	18.70	69.60	11.70	0.94	178.04	67.49	22.37	0.46

Note: The specific water capacity was calculated as under 0.1 hPa intervals.

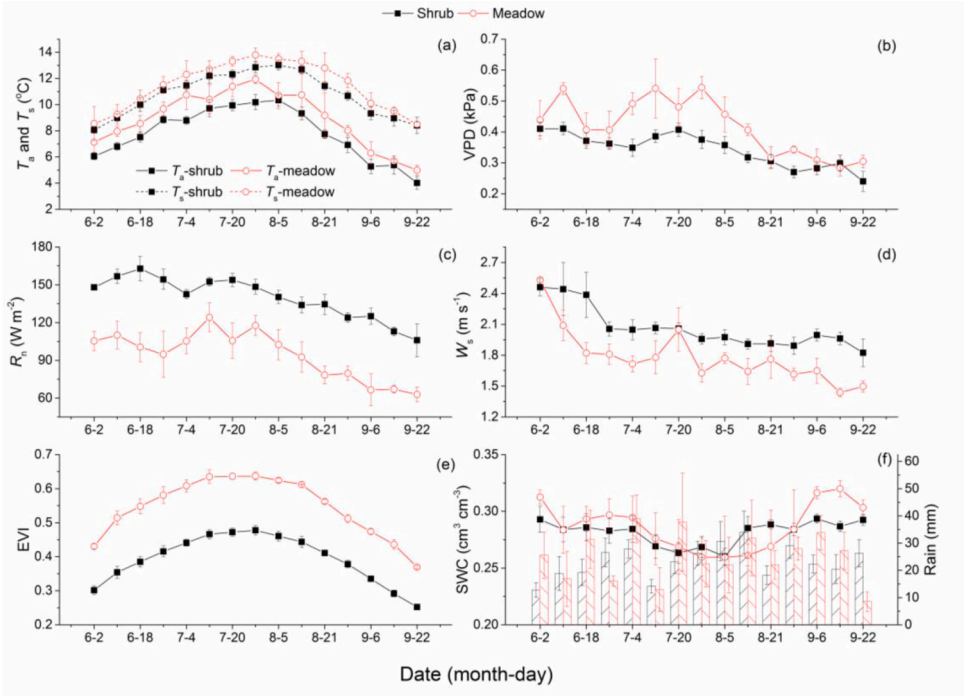

Fig. 1. Mean seasonal variations of air and topsoil temperature (T_a and T_s, a), vapor pressure deficit (VPD, b), net radiation (R_n, c), 2.2 m wind speed (W_s, d), enhanced vegetation index (EVI, e), volumetric 10 cm soil water content (SWC, f), and precipitation (Rain, f) in the shrub and the meadow (error bars are 1 standard deviation, the same below).

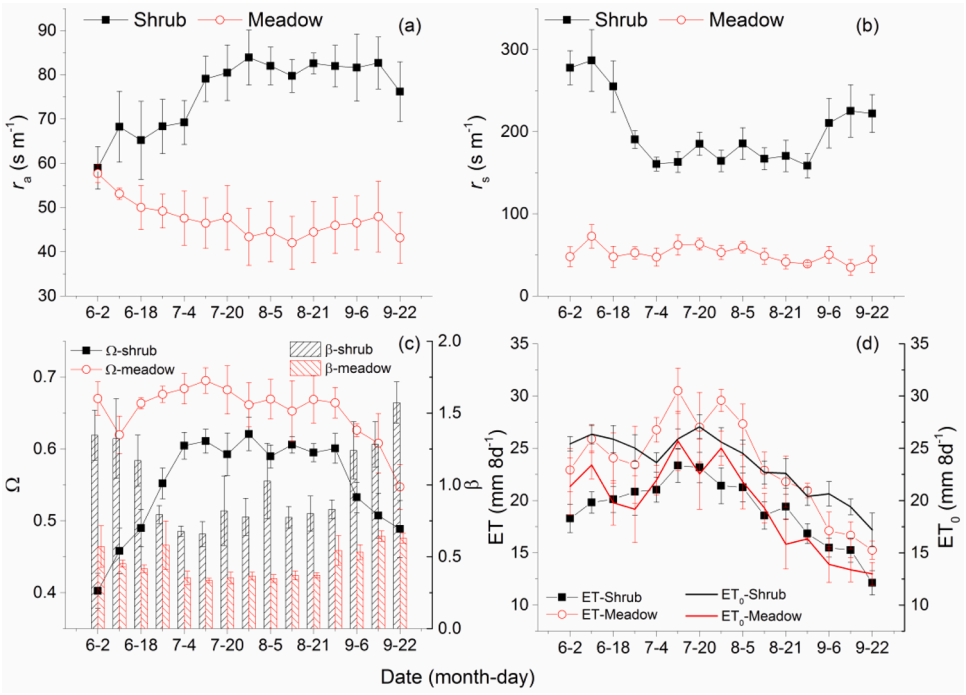

Fig. 2. Mean seasonal variations of aerodynamic resistance (r_a, a), bulk surface resistance (r_s, b), decoupling coefficient (Ω, c) and Bowen ratio (β, c), and evapotranspiration (ET, d) and reference ET (ET_0, d) in the shrub and the meadow.

replaced by those of a normal year). We then used a paired-samples t-test to detect differences in ET and in controls between the shrub and the meadow. Piecewise structural equation models (Piecewise SEM) have been widely used to piece together multiple separate linear models, to create a single casual network (Lefcheck, 2016). We constructed a Piecewise SEM from the Penman-Monteith Equation, as outlined in the schematic diagram in Fig. S4. The standardized path coefficients of the Piecewise SEM and total (direct and indirect) effects were reported to infer the relative importance of abiotic (R_n, VPD, T_a, T_s, SWC, W_s, Rain) and biotic (EVI) controls on ET. The 8-day data were used to fit the models in the R package 'piecewiseSEM' (Lefcheck, 2016), and model performance was evaluated using Shipley's test of d-separation (Fisher's

C) and Akaike's Information Criterion (AIC). Vegetation type was treated as a dummy variable, and the general linear model (GLM) was used to detect the effect of vegetation type on ET and the water supply (James et al., 2013). Conventional statistical analyses, such as linear regression and correlation analysis, were also implemented to provide insights into monthly and annual variations in ET and the water supply.

3. Results

3.1. Seasonal variability of abiotic and biotic controls

Fig. 1 showed that the seasonal variability for the main controls was similar at the two sites. T_a and VPD were 7.8 ± 2.0°C (mean ± SD, here and below) and 0.34 ± 0.06 kPa, respectively, for the upper shrub, which was significantly ($P < 0.001$) lower than for the lower meadow, where T_a and VPD were 8.9 ± 2.2°C and 0.42 ± 0.09 kPa, respectively (Fig. 1a, b). Topsoil temperature (T_s) averaged 10.8 ± 1.7°C in the shrub and 11.4± 1.9°C in the meadow, and the inter-site difference in T_s was lower than that in T_a. R_n and W_s were 32.6% and 12.1% higher for the shrub than for the meadow, respectively (Fig. 1c, d). There was a V-shaped seasonal trend in SWC, which both averaged 0.28 cm^3 cm^{-3}, and corresponded to a coefficient of variation of 3.8% for the shrub, and of 7.2% for the meadow. At the two sites, the minimum SWC occurred in early July, and was around 0.26 cm^3 cm^{-3}, which exceeds the soil wilting water content (Table 1). The mean warm-season precipitation in the shrub was 349.4 ± 6.0 mm, which was insignificantly ($P = 0.22$) lower than 374.7 ± 8.9 mm for the meadow. EVI peaked in late July, at 0.48 ± 0.01 and 0.64 ± 0.01 for the shrub and the meadow, respectively, when temperatures were warm.

3.2. Intra- and inter-annual variations in r_a, r_s, ET and ET_0

Warm-season r_a averaged 76.0 s m^{-1} with an increasing seasonal trend in the shrub while it was 47.3 s m^{-1} with a declining trend in the meadow (Fig. 2). The average r_s in the shrub was 201.8 ± 43.6 s m^{-1}, which was around four times larger than the average r_s (51.1 ± 10.0 s m^{-1}) in the meadow. The peak monthly ET was 89.0 ± 3.0 mm in the shrub, and 113.9 ± 2.6 mm in the meadow, and the peak occurred in July at both sites. The average monthly ET (ET_0) was 71.8 ± 10.1 mm (88.1 ± 3.1 mm) for the upper shrub, and 88.1 ± 6.3 mm (73.1 ± 5.6 mm) for the lower meadow. r_a was around 50% smaller than r_a calculated from the FAO-56 methods (109.1 s m^{-1} with a constant canopy height of 0.15 m) and this likely contributed to the fact that ET exceeded ET_0 in the meadow. The normalized ET (ET/ET_0) averaged 0.81 ± 0.01 in the shrub and 1.22 ± 0.02 in the meadow. The seasonal change in β was opposite of the seasonal change in ET at both sites; β averaged 1.01 ± 0.29 for the shrub and 0.46 ± 0.11 for the meadow. The decoupling coefficient for the shrub was 0.55 ± 0.07, which was significantly ($P <$ 0.001) lower than for the meadow, where it was 0.65 ± 0.04, suggesting a strong link between water loss and energy exchange over the meadow. The annual warm-season ET was 287.0 ± 17.6 mm in the shrub and 352.2 ± 15.7 mm in the meadow.

The Piecewise SEMs on the 8-day ET data were identified with Fisher's C < 21.4 and $P > 0.15$ (note that models where $P < 0.05$ were rejected). These models showed that, at both sites, R_n corresponded to a stronger standardized path coefficient than VPD did, and therefore influenced variations in ET more (Fig. 3). The total effect (direct + indirect) of R_n reached 0.59 (0.42 + 0.45 × 0.38) of the shrub and were more than 0.88 (0.64 + 0.72 × 0.34) of the meadow. This indicated that different mechanisms for translating the net radiation into a latent heat flux between the two sites. The general linear models also confirmed this difference by showing that R_n interacted significantly with vegetation type (as a category variable) on ET variability (Table 2). The influence of EVI and VPD on ET was similar for the two vegetation types (Table 2, Fig. S5). It should be noted that r_a had little direct effect on ET, but that r_s had a significant impact on ET in the shrub, indicating that there were

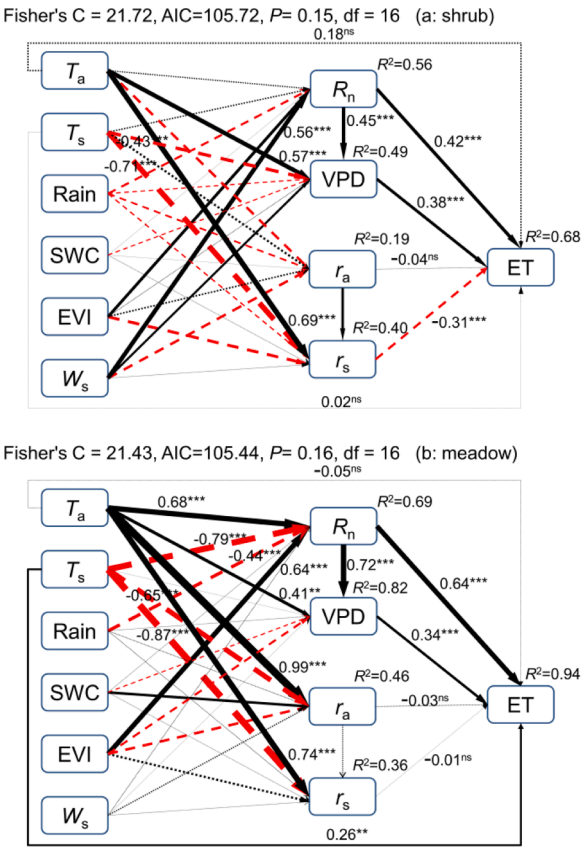

Fig. 3. Piecewise SEM models for the 8-day ET of the shrub (a) and the meadow (b). Black solid (red dashed) lines showed positive (negative) relationships; dotted lines showed that relationships were not statistically significant. The numbers that annotate the arrows were the standardized path coefficients, with significance levels indicated by ns ($P > 0.05$), * ($P < 0.05$), ** ($P < 0.01$), and *** ($P < 0.001$). For legibility, the coefficients for statistically significant indirect paths on ET were not shown if they were less than 0.40. R^2 showed the proportion of the total variance that was explained by the model. The weight for each line was ten times the standardized coefficient. Abbreviations: ET: evapotranspiration; R_n: net radiation; VPD: saturated vapor pressure deficit; r_a: aerodynamic resistance, r_s: bulk surface resistance; T_a: air temperature; T_s: soil temperature; SWC: volumetric soil water content; Rain: rainfall; W_s: wind velocity; EVI: enhanced vegetation index.

different ecophysiological controls for water loss between the two sites (Fig. 3). The stepwise linear regression showed that EVI had the strongest influence on monthly ET variability at both sites ($R^2 > 0.64$, $P <$ 0.001, Table S1). The bivariate correlation analysis showed that annual VPD was the sole driver for variations in annual ET in the meadow ($P =$ 0.013, $N = 4$, Table S2). There were non-significant relationships between annual ET and annual controls in the shrub ($P > 0.10$, $N = 10$, Table S2).

The bivariate correlation analysis of differences in the average 8-day ET and differences in the average controls (R_n, VPD, EVI, T_a, T_s, Ws, Rain, SWC, r_a, and r_s) between the two sites, showed that differences in R_n and in VPD significantly affected those in ET ($P < 0.001$, Table S3). The GLM analysis further showed that only the differences in VPD significantly accounted for 56% variations of the differences in ET between the shrub and the meadow ($R^2 = 0.85$, $P < 0.001$, N = 15). The differences in the average β between the two sites were largely controlled by differences in r_s (Fig. 4). T_s, rather than SWC, had a significant effect on r_s (Fig. 3), and therefore contributed significantly to the difference between the averaged β for the two sites (Fig. S6). The 8-day ET/ET_0 at the two sites were largely controlled by r_s and EVI, which were related to the ratio with a decreasing logarithmic relationship and an increasing linear relationship, respectively (Fig. 5). Some

Table 2
The analysis of variance from the general linear model of seasonal 8-day, monthly and yearly evapotranspiration (ET) with main controls (R_n, VPD, EVI) and vegetation types (Vege, categorical variable) during the warm-season in the shrub and in the meadow.

Dependant	Factors	df	Mean squares	*P* value	R^2
8-day ET	R_n	1	973.8	$P < 0.001$	0.64
	Vege	1	3250.4	$P < 0.001$	
	Rn × Vege	1	60.4	$P = 0.02$	
	Error	206	11.3		
	VPD	1	3908.6	$P < 0.001$	0.60
	Vege	1	75.6	$P = 0.02$	
	VPD × Vege	1	7.3	$P = 0.45$	
	Error	206	12.7		
	EVI	1	2286.4	$P < 0.001$	0.34
	Vege	1	10.3	$P = 0.19$	
	EVI × Vege	1	28.8	$P = 0.24$	
	Error	206	20.8		
Monthly ET	R_n	1	2505.7	$P < 0.001$	0.64
	Vege	1	15555.8	$P < 0.001$	
	Rn × Vege	1	320.1	$P = 0.19$	
	Error	52	179.2		
	VPD	1	18394.1	$P < 0.001$	0.64
	Vege	1	7.9	$P = 0.83$	
	VPD × Vege	1	21.8	$P = 0.73$	
	Error	52	178.4		
	EVI	1	15733.0	$P < 0.001$	0.62
	Vege	1	1710.5	$P = 0.004$	
	EVI × Vege	1	383.5	$P = 0.16$	
	Error	52	189.9		
Yearly ET	R_n	1	10102.4	$P < 0.001$	0.72
	Vege	1	2221.3	$P = 0.03$	
	Rn × Vege	1	28.1	$P = 0.78$	
	Error	10	331.5		
	VPD	1	10719.3	$P < 0.001$	0.77
	Vege	1	1922.6	$P = 0.02$	
	VPD × Vege	1	285.6	$P = 0.33$	
	Error	146	274.0		
	EVI	1	10408.4	$P < 0.001$	0.77
	Vege	1	1969.2	$P = 0.02$	
	EVI × Vege	1	492.3	$P = 0.21$	
	Error	146	279.7		

autocorrelation should be expected between r_s and ET, because of the mathematical dependency in Eq (3), however the rank for the correlation between ET/ET_0 and r_s was markedly lower for the meadow than for the shrub, also highlighting that r_s was important for water vapor transfer in the shrub.

3.3. Intra- and inter-annual variations in water supply

The transition of the cumulative water supply from a sink to a source occurred in late July in the shrub, and in late August for the meadow (Fig. 6). The monthly water supply was almost neutral during June and July, with values of 0.3 ± 7.8 mm for the shrub and –4.3 ± 19.4 mm for the meadow (Fig. 6). The peak monthly water supply occurred in August for the shrub, with a value of 35.7 ± 11.1 mm, and in September for the meadow, with a value of 20.4 ± 8.6 mm. Monthly precipitation, rather than monthly ET, determined the seasonal variability of the water supply, and the slope was similar at both sites, with a gradient of around one (Fig. 7). The GLM relating the monthly water supply to monthly precipitation and category variables (month or vegetation type), confirmed that the effects of season or vegetation type on the seasonal water supply were insignificant (Table S4).

The annual warm-season water supply was 62.4 ± 15.9 mm for the shrub and 22.5 ± 32.5 mm for the meadow. Annual precipitation, rather than annual ET, accounted for 85.0% of the inter-annual variability in the water supply (Fig. 8; Table S5). The linear slope between precipitation and the water supply was approximately one for both the annual and seasonal data (Figs.7, 8). This suggested that the proportion of precipitation that became part of the water supply remained constant, irrespective of temporal scales and vegetation types.

4. Discussion

4.1. The atmospheric evaporative demand on ET

Our results showed that atmospheric evaporative demand (vapor pressure deficit and radiation energy availability) was the principal contributor to variability in the 8-day ET at both sites (Fig. 3), which agreed with previous studies that humid alpine ecosystems are demand-limited (Liljedahl et al., 2011; Knowles et al., 2012; Zhu et al., 2014; Zhang et al., 2016). This stemmed from the fact that there were ample water supply (Zhang et al., 2018), small water vapor deficit (Körner, 2003), and comparable net radiation received despite high incoming solar radiation (Gupta et al., 1999). The positive effect of VPD on ET was associated with a low level of atmospheric drying (maximum incident VPD was about 2.0 kPa) that could stimulate canopy evapotranspiration, but not to the extent that plant stomata would close (Körner, 2003), although the slope for the relationship between VPD and ET was slightly shallower for the shrub than for the meadow (Table 2; Fig. 3). The differences in VPD thus explained the differences of ET between the shrub and the meadow (Table S3). Wind velocity was insignificantly related to ET at both sites (Fig. 3) because ET was decoupled from the atmosphere (the decoupling coefficient was greater than 0.5).

The available radiation energy, R_n, did have a positive effect on ET, but the shallow gradient of the slope between ET and R_n contributed to the fact that greater radiation absorption did not result in more ET in the shrub (Fig. 3; Table 2). This indicated that different mechanisms for converting radiative energy to ET were prevalent at the two sites (Baldocchi et al., 2004; Liljedahl et al., 2011; Zhang et al., 2016; Zeng et al., 2017). The most likely explanation for this came from the difference in the energy partitioning strategy, β, which was 1.01 for the shrub, and 0.46 for the meadow (Wilson et al., 2002). β is a function of atmospheric evaporative demand, aerodynamic resistance, surface resistance, and air temperature (Eq. (2); Wilson et al., 2002; Chapin et al., 2011). The climate at the two sites was similar, and so differences in aerodynamic resistance and in atmospheric demand (which is proportional to the ratio of VPD to R_n) should not explain the difference in β (Fig. 4; Wilson et al., 2002; Wieser et al., 2008; Liljedahl et al., 2011). The difference in β could thus be significantly attributed to the large difference in r_s for the two sites (Fig. 4; Wilson et al., 2002). At the shrub site, r_s was much higher than the meadow site, and was comparable to values that have been reported for other moist alpine shrub sites (Konzelmann et al., 1997; McFadden et al., 2003; Gu et al., 2005). The logarithmically decreasing curve that relates ET/ET_0 to r_s (Fig. 5), and the low value for the decoupling coefficient between ET/ET_0 and r_s (Fig. 2), also suggested that ET was strongly affected by r_s. These consistently indicated that the ecophysiological control (r_s) constrained the conversion of net radiation into latent heat over relatively dry surfaces in the shrub (Humphreys et al., 2006; Baldocchi and Xu, 2007; Gu et al., 2008; Liljedahl et al., 2011; Zhu et al., 2014).

4.2. The relationship between r_s and vegetation type

Conceptually, r_s captures the resistance of water vapor transfer from canopy and soil (Wilson et al., 2002; Chapin et al., 2011). Topsoil

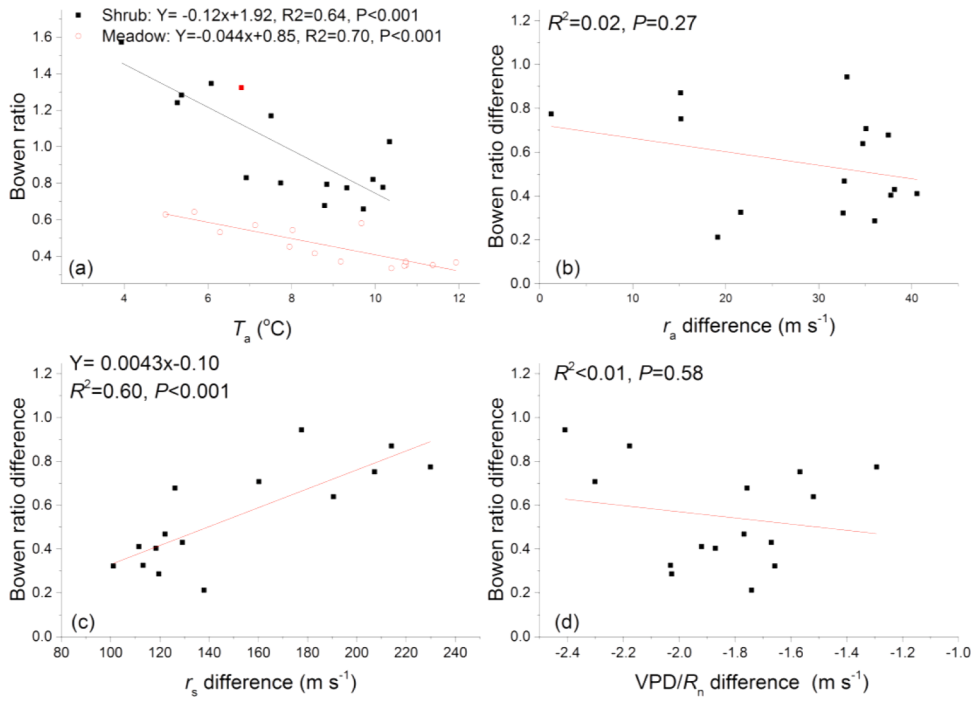

Fig. 4. The relationship between the 8-day average Bowen ratio and the average air temperature (T_a) in the shrub and in the meadow(a). The difference of the average 8-day Bowen ratio against the difference of the average 8-day aerodynamic resistance (r_a, b), the difference of the average 8-day bulk surface resistance (r_s, c), and the difference of the average 8-day atmospheric evaporative demand (VPD/R_n, d) between the shrub and the meadow.

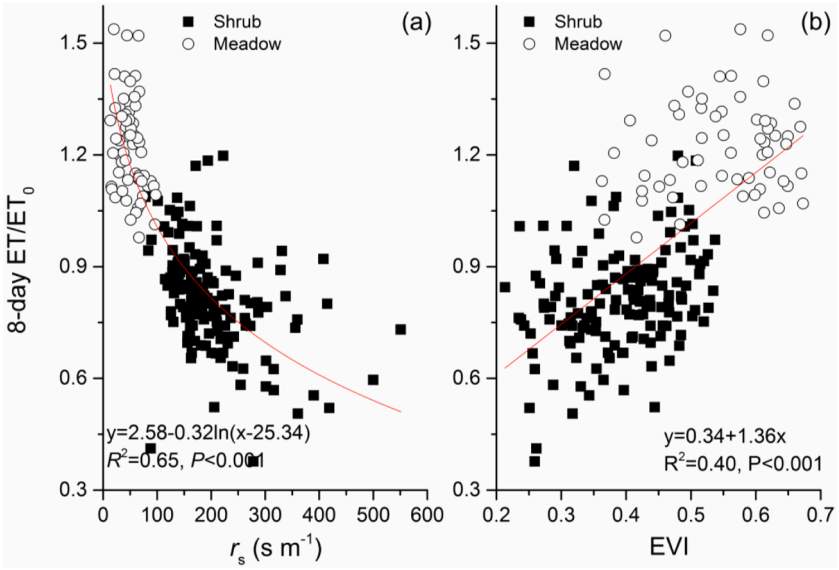

Fig. 5. Relationship between 8-day ET/ET$_0$ with buck surface resistance (r_s, a) and enhanced vegetation index (EVI, b) of the shrub and the meadow.

resistance was usually expressed as an exponential function of the soil water content (Hu et al., 2009; Zhang et al., 2018), which meant that it may average 221.6 ± 3.3 s m^{-1} for the shrub and 477.4 ± 2.5 s m^{-1} for the meadow. If the topsoil resistance was lower for the shrub than for the meadow, then it could not be driving the higher r_s for the shrub. The difference between r_s at the two sites should therefore stem from a difference in the canopy resistance (Baldocchi et al., 2004) (i.e., the maximum stomatal conductance and effective leaf areas). The stomatal conductance was strongly linked to maximum canopy photosynthetic capacity (A_{max}) in humid conditions, which was derived from the rectangular hyperbolic Michiaelis-Menten light-response function to be ca. 0.84 mg CO_2 m^{-2} s^{-1} for the shrub and 1.34 mg CO_2 m^{-2} s^{-1} for the meadow (Li H et al., 2014). When A_{max} was normalized by leaf area, it became 0.336 mg CO_2 m^{-2} s^{-1} for the shrub, and 0.343 mg CO_2 m^{-2} s^{-1} for the meadow. This, and the fact that there was no magnitude difference in the maximum conductance for the dominant alpine plant species (Kelliher et al., 1993; 1995; Rydsaa et al., 2015; Table S6), suggested that the maximum stomatal conductance was unlikely to explain the difference in r_s between the two sites. The different leaf areas and associated moss abundances (Blok et al., 2011; Anderegg et al., 2018; Li et al., 2019) may therefore contribute to r_s being higher for the shrub than for the meadow.

r_s scales negatively with leaf area (Baldocchi et al., 2004; Peng et al., 2019), and the difference between the 8-day average MODIS-LAI could

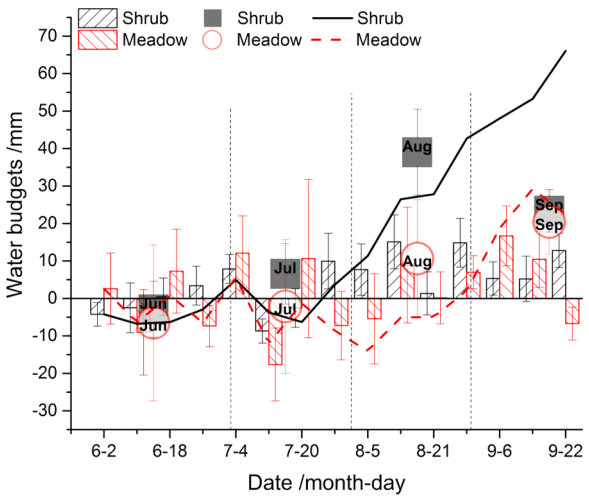

Fig. 6. Seasonal variability in water supply for the shrub and for the meadow (The large symbols were the mean monthly value; the line showed the cumulative 8-day water supply).

account for 41% of the between-site variability in r_s ($P = 0.006$, $N = 15$), however LAI affected r_s differently at the two sites. Specifically, the averaged 8-day r_s was negatively correlated with the averaged 8-day MODIS-LAI for the shrub via an asymptotic function ($r_s = 195.83 - 45.38 \times \ln(\text{LAI} - 0.2)$, $R^2 = 0.49$, $P = 0.007$, Fig. S7). Conversely, in the meadow, VPD explained most of the seasonal variability in r_s ($R^2 = 0.72$, $P < 0.001$, Fig. S7), and very little of it could be attributed to MODIS-LAI ($R^2 < 0.01$, $P = 0.50$). This divergence suggested that the direct effect of leaf areas on water vapor conductance may be constrained under the lower plant coverage (LAI below ca. 1.5 $m^2 \bullet m^{-2}$). Moss often covered a large proportion of the ground surface and shrub stems, where the vegetation canopy is less dense during the warm-season at humid alpine sites (Eugster et al., 2002; Blok et al., 2011). The surface resistance to water loss increases exponentially for moss as the tissue water content decreases (McFadden et al., 2003; Humphreys et al., 2006; Blok et al., 2011; Liljedahl et al., 2011), and so a higher moss abundance induced by lower vascular plant coverage probably contributed to r_s being higher for the shrub than for the meadow. This was partly confirmed by the insignificance of the correlation between r_s and VPD for the shrub ($R^2 < 0.01$, $P = 0.61$, Fig. S7). It was therefore likely that the relationship between ET and shrub expansion from numerical modeling (Rydsaa et al., 2015) and from a micro-lysimeter experiment (Blok et al., 2011), differ because of the significant contribution that cryptogam abundance makes to the bulk surface resistance. The direct (stomatal conductance)

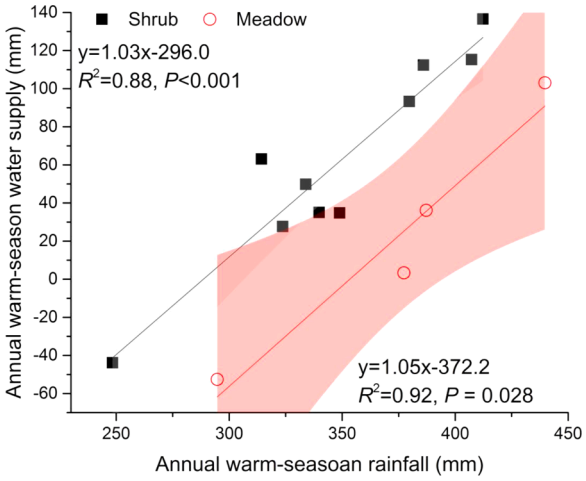

Fig. 8. The relationship between the annual water supply and annual precipitation during the warm-season in the shrub and in the meadow. Shaded areas showed the 95% confidence of the regression line.

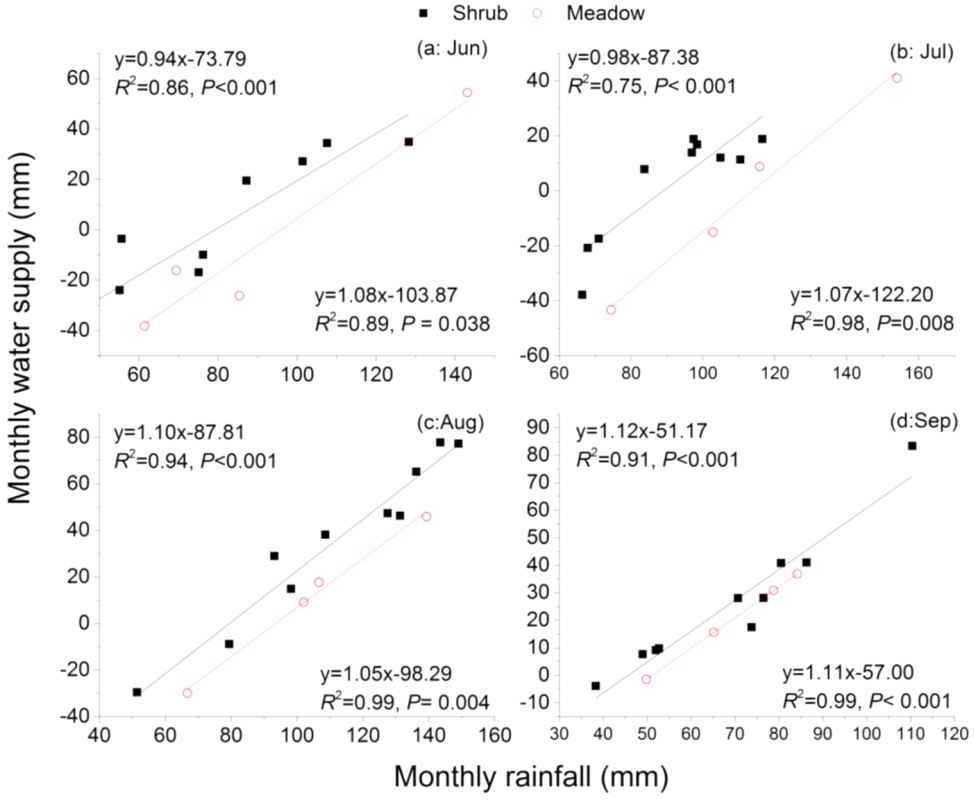

Fig. 7. The relationship between the monthly water supply and monthly precipitation in the shrub and in the meadow (June: a, July: b, August: c, September: d).

and indirect (moss abundance) effects of vegetation growth on r_s explained the variability for energy partitioning β (Fig. 4; Gu et al., 2005; 2008; Liu et al., 2009; Li et al., 2019). Nevertheless, other physiological factors, such as apparent individual leaf stomatal resistance and water use strategy (Teuling et al., 2010), and non-physiological factors, such as mathematically dependent aerodynamic resistance (Chapin et al., 2011), should also be considered when further assessing energy partitioning.

P. fruticosa has a small leaf area, a thin leaf boundary layer, and a relatively open canopy structure, which all contributed to the effective convection of sensible heat (Baldocchi and Xu, 2007). The average daily-integrated sensible heat flux was 3.5 MJ•day^{-1} for the shrub, and 2.0 MJ•day^{-1} for the meadow, and this difference also contributed to β being higher for the shrub than the meadow. In summary, the energy partitioning strategy, which was determined by the surface resistance and canopy structure, could explain why ET was not higher in the shrub than the meadow, despite the higher available radiation energy in the shrub. This supported our hypothesis that vegetation type could exert a significant influence on ET dynamics, although ET is primarily influenced by the availability of radiation energy in humid sites.

4.3. Consistent water supply

The water balance in the warm-season was primarily regulated by precipitation, evapotranspiration, soil water storage, and glacier melt in alpine regions (Biskop et al., 2016). However, monthly and annual variations in the water supply were more strongly positively correlated with precipitation than with ET at the two sites (Figs.4, 5; Table S5). This supported the finding that precipitation was the primary driver for variability in runoff under humid alpine climates (Humphreys et al., 2006; Cui et al., 2009; Zuo et al., 2016). The two humid sites acted as water sinks in June and July, and as water sources in August and September, when there was river flooding (Wang et al., 2009), and endorheic lake levels increased (Biskop et al., 2016) on the Qinghai-Tibetan Plateau. The dominant role of precipitation in driving the water supply was probably related to the conservative ET and the high seasonality for precipitation, as well as to small seasonal changes in soil water storage at both sites. The coefficients of variance (CV) for the monthly and annual ET at the shrub and meadow sites averaged 12.4%, 5.8% and 5.9%, 4.5%, respectively, compared with CVs for monthly and annual precipitation at the shrub and meadow sites of 28.3%, 13.7% and 30.3%, 16.0%, respectively. Previous studies of humid alpine areas have also reported similarly uniform values for ET (Wieser et al., 2008; Hu et al., 2009; Liljedahl et al., 2011). The range in average topsoil water content (maximum minus minimal) for the shrub and the meadow was only 0.03 cm^3 cm^{-3} and 0.06 cm^3 cm^{-3} (Fig. 1), respectively, which suggested that the topsoil water storage was in a relatively steady-state and would not have substantially affected the water balance. The similarity of the slopes for the relationship between water supply and precipitation at the two sites highlighted that a consistent proportion of precipitation became water yield, provided that the relatively constant evaporative demand was met (Figs.4, 5). These findings agreed with other works, which have reported that precipitation played the dominant role in the regional water yields in humid regions (Wieser et al., 2008; Cui et al., 2009; Biskop et al., 2016).

4.4. Effects of shrub expansion on ET and water supply

Our results indicated that shrub expansion into areas of alpine meadows (Eugster et al., 2002; Klein et al., 2007) would result in increased regional water supply under current precipitation regimes (Yang et al., 2012). This probably stemmed from the different energy partitioning strategies and surface resistances of the two vegetation types (Wilson et al., 2002). The multi-storied structure of the alpine shrub led to it having a lower surface albedo of 0.12 than 0.18 of the alpine meadow (Eugster et al., 2002; Baldocchi et al., 2004; Liu et al., 2009). The higher net radiation received by areas vegetated with alpine shrub could stimulate stronger sensible heat than latent heat, because of the lower Bowen ratio of the alpine shrub, relative to the alpine meadow (Fig. 2). Although aerodynamic resistance was higher for the alpine shrub than for the alpine meadow, it had little effect on ET variability (Fig. 3), and so the impact of shrub expansion on the water cycle, via changes in surface roughness, may be insignificant (Sterling et al., 2013). The bulk surface resistance (Fig. 2) and the more conservative water use strategy (Teuling et al., 2010) may reduce ET for areas of alpine shrub, relative to areas of alpine meadow. However, the lower Bowen ratio was closely linked to a higher bulk surface resistance (Fig. 4), probably because of moss coverage, more than shrub abundance (Table S6). If the open canopy architecture and relatively high moss coverage were substantially reduced in the colonizing shrub at lower elevations, then the expansion of alpine shrub into areas of meadow would exert little influence on regional energy exchange and water supply (Rydsaa et al., 2015). Soil water content and specific water capacity were 68.1% and 144.1% higher, respectively, for the shrub than for the meadow. The soil wilting water content was very close between the two sites (Table 1), which suggested that shrub expansion could substantially affect soil water holding capacity, provided that soil properties for the area colonized by the shrub are the same as those for the measured shrub area. In summary, shrub expansion into areas of meadows could improve the magnitude and stability of the regional water supply by reducing ET loss and enhancing the soil water holding capacity.

5. Conclusions and implications

ET was primarily driven by the available radiative energy and vapor pressure deficit at both humid alpine sites. ET was lower in the upper shrub than in the lower meadow, despite the shrub being associated with higher net radiation absorption. This was mainly due to the higher bulk surface resistance, and the consequently higher Bowen ratio, for the shrub. The difference in the surface resistances between the shrub and the meadow resulted from differences in the plant leaf areas and potential moss abundance. The monthly and annual water supply was determined by variable precipitation, rather than by conservative ET, which resulted in a consistent proportion of precipitation being incorporated into the water supply at both sites.

Our results have important implications for understanding the spatiotemporal variability of water supply in alpine regions. The bulk surface resistance and energy partitioning strategy for alpine shrub were distinct from those for alpine meadow, which results in lower ET and higher water yields for shrub areas. However, shrub expansion into meadow areas may degrade forage production because shrubs produce less digestible forage than meadows, and so a balance between water supply and rangeland quality may be required.

Author contributions

H Li, F Zhang, and Zhu J carried out all analyses. Y Li and G Cao conceived the manuscript. All authors collaborated in the interpretation of the results and the writing of the paper.

Declaration of Competing Interest

The authors declare no conflict of interest.

Acknowledgments

This work was funded by the National Key R&D Program (2017YFA0604801), the National Natural Science Foundation of China (41730752, 41877547), Qinghai R&D Infrastructure and Facility Development Program (2018-ZJ-T09), Qinghai Innovation Platform Construction Project (2017-ZJ-Y20), and the Chinese Academy of

Sciences-People's Government of Qinghai Province Joint Grant on Sanjiangyuan National Park Research (YHZX-2020-07).

Supplementary materials

Supplementary material associated with this article can be found, in the online version, at doi:10.1016/j.agrformet.2021.108318.

References

ACIA, 2004. Impacts of a Warming Arctic: Arctic Climate Impact Assessment. Cambridge University Press, Cambridge, UK.

Allen, R.G., Periera, L.S., Raes, D., Smith, M., 1998. Crop evapotranspiration: Guidelines for Computing Crop Requirements. Irrigation and Drainage paper NO.56. FAO, Rome, Italy, p. 300.

Anderegg, W.R.L., Konings, A.G., Trugman, A.T., Yu, K., Bowling, D.R., Gabbitas, R., Karp, D.S., Pacala, S., Sperry, J.S., Sulman, B.N., Zenes, N., 2018. Hydraulic diversity of forests regulates ecosystem resilience during drought. Nature 561, 538–541. https://doi.org/10.1038/s41586-018-0539-7.

Baldocchi, D.D., Xu, L., 2007. What limits evaporation from Mediterranean oak woodlands – the supply of moisture in the soil, physiological control by plants or the demand by the atmosphere? Adv. Water Resour. 30, 2113–2122. https://doi.org/10.1016/j.advwatres.2006.06.013.

Baldocchi, D.D., Xu, L., Kiang, N., 2004. How plant functional-type, weather, seasonal drought, and soil physical properties alter water and energy fluxes of an oak-grass savanna and an annual grassland. Agr. Forest. Meteorol. 123, 13–39. https://doi.org/10.1016/j.agrformet.2003.11.006.

Biskop, S., Maussion, F., Krause, P., Fink, M., 2016. Differences in the water-balance components of four lakes in the southern-central Tibetan Plateau. Hydrol. Earth Syst. Sc. 20, 209–225. https://doi.org/10.5194/hess-20-209-2016.

Blok, D., Heijmans, M.M.P.D., Schaepman-Strub, G., van Ruijven, J., Parmentier, F.J.W., Maximov, T.C., Berendse, F., 2011. The cooling capacity of mosses: controls on water and energy fluxes in a Siberian Tundra Site. Ecosystems 14, 1055–1065. https://doi.org/10.1007/s10021-011-9463-5.

Brümmer, C., Black, T.A., Jassal, R.S., Grant, N.J., Spittlehouse, D.L., Chen, B., Nesic, Z., Amiro, B.D., Arain, M.A., Barr, A.G., Bourque, C.P.A., Coursolle, C., Dunn, A.L., Flanagan, L.B., Humphreys, E.R., Lafleur, P.M., Margolis, H.A., McCaughey, J.H., Wofsy, S.C., 2012. How climate and vegetation type influence evapotranspiration and water use efficiency in Canadian forest, peatland and grassland ecosystems. Agr. Forest. Meteorol. 153, 14–30. https://doi.org/10.1016/j.agrformet.2011.04.008.

Chapin, F.S., Matson, P.A., Mooney, H.A., 2011. Principles of Terrestrial Ecosystem Ecology. Springer-Verlag, New York, USA, pp. 142–145.

Chen, R.S., Kang, E.S., Ji, X.B., Yang, J.P., Yang, Y., 2006. Cold regions in China. Cold Reg. Sci. Technol. 45, 95–102. https://doi.org/10.1016/j.coldregions.2006.03.001.

Cui, J., An, S., Wang, Z., Fang, C., Liu, Y., Yang, H., Xu, Z., Liu, S., 2009. Using deuterium excess to determine the sources of high-altitude precipitation: implications in hydrological relations between sub-alpine forests and alpine meadows. J. Hydrol. 373, 24–33. https://doi.org/10.1016/j.jhydrol.2009.04.005.

Eugster, W., Rouse, W.R., Pielke Sr, R.A., Mcfadden, J.P., Baldocchi, D.D., Kittel, T.G.F., Chapin, F.S., Liston, G.E., Vidale, P.L., Vaganov, E., Chambers, S., 2002. Land–atmosphere energy exchange in Arctic tundra and boreal forest: available data and feedbacks to climate. Global Change Biol. 6, 84–115. https://doi.org/10.1046/j.1365-2486.2000.06015.x.

Gu, S., Tang, Y., Cui, X., Du, M., Liang, Z., Li, Y., Xu, S., Zhou, H., Kato, T., Qi, P., 2008. Characterizing evapotranspiration over a meadow ecosystem on the Qinghai-Tibetan Plateau. J. Geophys. Res.-Atmos. 113 https://doi.org/10.1029/2007JD009173.

Gu, S., Tang, Y., Cui, X., Kato, T., Du, M., Li, Y., Zhao, X., 2005. Energy exchange between the atmosphere and a meadow ecosystem on the Qinghai-Tibetan Plateau. Agr. Forest. Meteorol. 129, 175–185. https://doi.org/10.1016/j.agrformet.2004.12.002.

Gupta, S.K., Ritchey, N.A., Wilber, A.C., Whitlock, C.H., Gibson, G.G., Stackhouse, P.W. J., 1999. A climatology of surface radiation budget derived from satellite data. J. Climate 12, 2691–2710.

Hammerle, A., Haslwanter, A., Tappeiner, U., Cernusca, A., Wohlfahrt, G., 2008. Leaf area controls on energy partitioning of a temperate mountain grassland. Biogeosciences 5, 421–431. https://doi.org/10.5194/bg-5-421-2008.

Hu, Z., Yu, G., Zhou, Y., Sun, X., Li, Y., Shi, P., Wang, Y., Song, X., Zheng, Z., Zhang, L., Li, S., 2009. Partitioning of evapotranspiration and its controls in four grassland ecosystems: application of a two-source model. Agr. Forest Meteorol. 149, 1410–1420. https://doi.org/10.1016/j.agrformet.2009.03.014.

Humphreys, E.R., Lafleur, P.M., Flanagan, L.B., Hedstrom, N., Syed, K.H., Glenn, A.J., Granger, R., 2006. Summer carbon dioxide and water vapor fluxes across a range of northern peatlands. J. Geophys. Res.-Biogeo. 111 https://doi.org/10.1029/2005JG000111.

James, G., Witten, D., Hastie, T., Tibshirani, R., 2013. An Introduction to Statistical Learning- with Applications in R. Springer-Verlag, New York, USA.

Kelliher, F.M., Leuning, R., Raupach, M.R., Schulze, E.D., 1995. Maximum conductances for evaporation from global vegetation types. Agr. Forest Meteorol. 73, 1–16. https://doi.org/10.1016/0168-1923(94)02178-M.

Kelliher, F.M., Leuning, R., Schulze, E.D., 1993. Evaporation and canopy characteristics of coniferous forests and grasslands. Oecologia 95, 153–163. https://doi.org/10.1007/BF0032348.

Klein, J., Harte, J., Zhao, X., 2007. Experimental warming, not grazing, decreases rangeland quality on the Tibetan Plateau. Ecol. Appl. 17, 541–557. https://doi.org/10.1890/05-0685.

Knowles, J.F., Blanken, P.D., Williams, M.W., Chowanski, K.M., 2012. Energy and surface moisture seasonally limit evaporation and sublimation from snow-free alpine tundra. Agr. Forest Meteorol. 157, 106–115. https://doi.org/10.1016/j.agrformet.2012.01.017.

Konzelmann, T., Calanca, P., Müller, G., Menzel, L., Lang, H., 1997. Energy balance and evapotranspiration in a high mountain area during summer. J. Appl. Meteorol. 36, 966–973. https://doi.org/10.1175/1520-0450(1997)0362.0.CO;2.

Körner, C., 2003. Alpine Plant Life: Functional Plant Ecology of High Mountain Ecosystems. Springer-Verlag, Berlin Heidelberg.

Lefcheck, J.S., 2016. piecewiseSEM: Piecewise structural equation modelling in r for ecology, evolution, and systematics. Methods Ecol. Evol. 7, 573–579. https://doi.org/10.1111/2041-210X.12512.

Li, H., Zhang, F., Li, Y., Cao, G., Zhao, L., Zhao, X., 2014. Seasonal and interannual variations of ecosystem photosynthetic features in an alpine dwarf shrubland on the Qinghai-Tibetan Plateau, China. Photosynthetica 52, 321–331. https://doi.org/10.1007/s11099-014-0035-8.

Li, H., Zhang, F., Li, Y., Wang, J., Zhang, L., Zhao, L., Cao, G., Zhao, X., Du, M., 2016. Seasonal and inter-annual variations in CO_2 fluxes over 10 years in an alpine shrubland on the Qinghai-Tibetan Plateau, China. Agr. Forest Meteorol. 228–229, 95–103. https://doi.org/10.1016/j.agrformet.2016.06.020.

Li, H., Zhang, F., Li, Y., Zhao, X., Cao, G., 2015. Thirty-year variations of above-ground net primary production and precipitation-use efficiency of an alpine meadow in the north-eastern Qinghai-Tibetan Plateau. Grass Forage Sci. 71, 208–218. https://doi.org/10.1111/gfs.12165.

Li, H., Zhu, J., Zhang, F., He, H., Yang, Y., Li, Y., Cao, G., Zhou, H., 2019. Growth stage-dependant variability in water vapor and CO_2 exchanges over a humid alpine shrubland on the northeastern Qinghai-Tibetan Plateau. Agr. Forest Meteorol. 268, 55–62. https://doi.org/10.1016/j.agrformet.2019.01.013.

Li, X., Wang, L., Chen, D., Yang, K., Wang, A., 2014. Seasonal evapotranspiration changes (1983–2006) of four large basins on the Tibetan Plateau. J. Geophys. Res.-Atmos. 119, 13079–13095. https://doi.org/10.1002/2014JD022380.

Liljedahl, A.K., Hinzman, L.D., Harazono, Y., Zona, D., Tweedie, C.E., Hollister, R.D., Engstrom, R., Oechel, W.C., 2011. Nonlinear controls on evapotranspiration in arctic coastal wetlands. Biogeosciences 8, 3375–3389. https://doi.org/10.5194/bg-8-3375-2011.

Liu, S., Li, S.G., Yu, G.R., Sun, X.M., Zhang, L.M., Hu, Z.M., Li, Y.N., Zhang, X.Z., 2009. Surface energy exchanges above two grassland ecosystems on the Qinghai-Tibetan Plateau. Biogeosci. Discuss 2009, 9161–9192. https://doi.org/10.5194/bgd-6-9161-2009.

McFadden, J.P., Eugster, W., Chapin, F.S., 2003. A regional study of the controls on water vapor and CO_2 exchange in arctic tundra. Ecology 84, 2762–2776. https://doi.org/10.1890/01-0444.

Monteith, J.L., 1965. Evaporation and environment. Symp. Soc. Exp. Biol. 19, 205–234.

Peng, L., Zeng, Z., Wei, Z., Chen, A., Wood, E.F., Sheffield, J., 2019. Determinants of the ratio of actual to potential evapotranspiration. Global Change Biol. 25, 1326–1343. https://doi.org/10.1111/gcb.14577.

Rydsaa, J.H., Stordal, F., Tallaksen, L.M., 2015. Sensitivity of the regional European boreal climate to changes in surface properties resulting from structural vegetation perturbations. Biogeosciences 12, 3071–3087. https://doi.org/10.5194/bg-12-3071-2015.

Shen, M., Piao, S., Jeong, S., Zhoue, L., Zeng, Z., Ciais, P., Chen, D., Huang, M., Jin, C., Li, L.Z.X., Li, Y., Myneni, R.B., Yang, K., Zhang, G., Zhang, Y., Yao, T., 2015. Evaporative cooling over the Tibetan Plateau induced by vegetation growth. P. Natl. Acad. Sci. USA 112, 9299–9304. https://doi.org/10.1073/pnas.1504418112.

Sterling, S.M., Ducharne, A., Polcher, J., 2013. The impact of global land-cover change on the terrestrial water cycle. Nat. Clim. Change 3, 385–390. https://doi.org/10.1038/nclimate1690.

Teuling, A.J., Seneviratne, S.I., Stockli, R., Reichstein, M., Moors, E., Ciais, P., Luyssaert, S., van den Hurk, B., Ammann, C., Bernhofer, C., Dellwik, E., Gianelle, D., Gielen, B., Grunwald, T., Klumpp, K., Montagnani, L., Moureaux, C., Sottocornola, M., Wohlfahrt, G., 2010. Contrasting response of European forest and grassland energy exchange to heatwaves. Nat. Geosci. 3, 722–727. https://doi.org/10.1038/ngeo950.

Wang, G., Hu, H., Li, T., 2009. The influence of freeze-thaw cycles of active soil layer on surface runoff in a permafrost watershed. J. Hydrol. 375, 438–449. https://doi.org/10.1016/j.jhydrol.2009.06.046.

Wieser, G., Hammerle, A., Wohlfahrt, G., 2008. The water balance of grassland ecosystems in the Austrian Alps. Arct Antarct. Alp. Res. 40, 439–445. https://doi.org/10.1657/1523-0430(07-039)[WIESER]2.0.CO;2.

Williams, C.A., Reichstein, M., Buchmann, N., Baldocchi, D., Beer, C., Schwalm, C., Wohlfahrt, G., Hasler, N., Bernhofer, C., Foken, T., Papale, D., Schymanski, S., Schaefer, K., 2012. Climate and vegetation controls on the surface water balance: Synthesis of evapotranspiration measured across a global network of flux towers. Water Resour. Res. 48, W06523. https://doi.org/10.1029/2011WR011586.

Wilson, K.B., Baldocchi, D.D., Aubinet, M., Berbigier, P., Bernhofer, C., Dolman, H., Falge, E., Field, C., Goldstein, A., Granier, A., Grelle, A., Halldor, T., Hollinger, D., Katul, G., Law, B.E., Lindroth, A., Meyers, T., Moncrieff, J., Monson, R., Oechel, W., Tenhunen, J., Valentini, R., Verma, S., Vesala, T., Wofsy, S., 2002. Energy partitioning between latent and sensible heat flux during the warm season at FLUXNET sites. Water Resour. Res. 38, 1294. https://doi.org/10.1029/2001WR000989.

Xiao, J., Sun, G., Chen, J., Chen, H., Chen, S., Dong, G., Gao, S., Guo, H., Guo, J., Han, S., Kato, T., Li, Y., Lin, G., Lu, W., Ma, M., McNulty, S., Shao, C., Wang, X., Xie, X.,

Zhang, X., Zhang, Z., Zhao, B., Zhou, G., Zhou, J., 2013. Carbon fluxes, evapotranspiration, and water use efficiency of terrestrial ecosystems in China. Agr. Forest Meteorol. 182–183, 76–90. https://doi.org/10.1016/j.agrformet.2013.08.007.

Xin, Y., Chen, F., Zhao, P., Barlage, M., Blanken, P., Chen, Y., Chen, B., Wang, Y., 2018. Surface energy balance closure at ten sites over the Tibetan plateau. Agr. Forest Meteorol. 259, 317–328. https://doi.org/10.1016/j.agrformet.2018.05.007.

Yang, Y., Xiao, H., Wei, Y., Zhao, L., Zou, S., Yang, Q., Yin, Z., 2012. Hydrological processes in the different landscape zones of alpine cold regions in the wet season, combining isotopic and hydrochemical tracers. Hydrol. Process 26, 1457–1466. https://doi.org/10.1002/hyp.8275.

Yao, T., Thompson, L.G., Mosbrugger, V., Zhang, F., Ma, Y., Luo, T., Xu, B., Yang, X., Joswiak, D.R., Wang, W., Joswiak, M.E., Devkota, L.P., Tayal, S., Jilani, R., Fayziev, R., 2012. Third pole environment (TPE). Environ. Dev. 3, 52–64. https://doi.org/10.1016/j.envdev.2012.04.002.

Zeng, Z., Piao, S., Li, L.Z.X., Zhou, L., Ciais, P., Wang, T., Li, Y., Lian, X., Wood, E.F., Friedlingstein, P., Mao, J., Estes, L.D., Myneni, R.B., Peng, S., Shi, X., Seneviratne, S. I., Wang, Y., 2017. Climate mitigation from vegetation biophysical feedbacks during the past three decades. Nat. Clim. Change 7, 432–436. https://doi.org/10.1038/nclimate3299.

Zhang, F., Li, H., Li, Y., Guo, X., Dai, L., Lin, L., Cao, G., Li, Y., Zhou, H., 2019. Strong seasonal connectivity between shallow groundwater and soil frost in a humid alpine meadow, northeastern Qinghai-Tibetan Plateau. J. Hydrol. 574, 926–935. https://doi.org/10.1016/j.jhydrol.2019.05.008.

Zhang, F., Li, H., Wang, W., Li, Y., Lin, L., Guo, X., Du, Y., Li, Q., Yang, Y., Cao, G., Li, Y., 2018. Net radiation rather than moisture supply governs the seasonal variations of evapotranspiration over an alpine meadow on the northeastern Qinghai-Tibetan Plateau. Ecohydrology 11, e1925. https://doi.org/10.1002/eco.1925.

Zhang, S., Li, X., Zhao, G., Huang, Y., 2016. Surface energy fluxes and controls of evapotranspiration in three alpine ecosystems of Qinghai Lake watershed, NE Qinghai-Tibet Plateau. Ecohydrology 9, 267–279. https://doi.org/10.1002/eco.1633.

Zheng, D., Zhang, Q.S., Wu, S.H., 2000. Mountain Geoecology and Sustainable Development of the Tibetan Plateau. Kluwer Academic, Dordercht, the Netherlands.

Zhu, G., Lu, L., Su, Y., Wang, X., Cui, X., Ma, J., He, J., Zhang, K., Li, C., 2014. Energy flux partitioning and evapotranspiration in a sub-alpine spruce forest ecosystem. Hydrol. Process. 28, 5093–5104. https://doi.org/10.1002/hyp.9995.

Zuo, Y., Wang, Q., Zheng, H., Shi, P., Li, Y., Wang, Y., 2016. Seasonal variations of the water budget in typical grassland ecosystems in China. Acta Ecol. Sin. 36, 301–310. https://doi.org/10.1016/j.chnaes.2016.06.003.